JOURNAL OF MATERIALS SCIENCE 27 (1992) 180–190

Alkali carbonation of autoclaved polymer–cement composites in Na_2CO_3-laden water at 300 °C

T. SUGAMA, G. GRAY*, L. E. KUKACKA
Energy Efficiency and Conservation Division, Department of Applied Science, Brookhaven National Laboratory, Upton, NY 11973, USA

Well cements resistive to high-temperature (~300 °C) brines containing carbon dioxide (CO_2) are needed for use in the completion of geothermal wells. Recent attempts to complete wells through aquifers containing ~1000 p.p.m. concentrations of CO_2 at ~130 °C have shown severe deterioration of all conventional cement systems, with resulting cement and casing failures after only 90 days in service. As part of an ongoing research programme to develop hydrothermally and CO_2-resistant cement formulations, studies were performed to determine the rate of alkali carbonation of autoclave-treated polymer–calcium aluminate cement composites upon exposure to Na_2CO_3-laden water at 300 °C. The results indicated that the formation of a calcium-complexed carboxylate polymer structure, resulting from the addition of an acrylic polymer in the cement, improved the compressive strength of the composite after a 1 day autoclave exposure, and minimized the carbonation rate over 30 days. However, biccholite→wairakite and triclinic→hexagonal anorthite transformations resulted in strength degradation after exposure for times up to 30 days. The polymer system found to be most effective for minimizing strength degradation and carbonation reactions was a carboxylated styrene–butadiene copolymer.

1. Introduction

Previous work at Brookhaven National Laboratory has indicated that the rate of carbonation of calcium silicate-based geothermal cementing materials due to exposure to CO_2-enriched fluids at temperatures ranging from 150–250 °C, is dependent upon the species of the calcium silicate hydrate phases formed in the hydrated cementitious materials [1–3]. It was found that the formation of xonotolite or truscottite produces stable phases which are highly resistive to carbonation. In contrast, the 1.1 nm tobermorite phase was found to be extremely vulnerable to attack by CO_2. The resultant transition of calcium hydroxide to calcite produces an effective network barrier which acts to prevent further penetration of CO_2. In addition, the presence of calcite formed in this initial carbonation process tends to increase the mechanical strength of the cement. Subsequently, strength retrogression occurs as a result of the *in situ* conversion of the calcite to water-soluble calcium bicarbonate. This process has been interpreted by Bruckdorfer [4], as follows. The converted calcium bicarbonate reacts with more calcium hydroxide to form calcium carbonate and, most importantly, fresh water which dissolves more calcium bicarbonate. This leaching process continues in the presence of excess CO_2, thereby producing a large amount of an amorphous silica gel dissociated from the crystalline calcium silicate hydrate compounds.

In our previous studies, CO_2 gas was dissolved in tap water rather than in a simulated geothermal brine. Therefore, because the sodium ion concentration in geothermal brines is high, it is important to determine if the decomposition of the cementing material after exposure to CO_2-laden hot brine is only due to severe carbonation of the hydrated cement products, or also as a result of alkali metal-catalysed hydrolysis of the cement hydrates caused by the attack of sodium cations.

The decomposition of hydrated high alumina cement resulting from the combined effects of carbonation and alkali metal hydrolysis was investigated by Midgley and Midgley [5]. They also reported the alkali carbonation reactions and kinetics for the alumina cement hydrates after soaking in alkali carbonate (such as Na_2CO_3, Li_2CO_3 and K_2CO_3) solutions at temperatures up to 40 °C [6, 7]. They reported that the surfaces of the hydrated cement specimens were very reactive with the alkali carbonate solutions, and that colloidal and gelatinous aluminate hydrates were formed as decomposition products.

Ideally, an inhibitor for minimizing alkali carbonation reactions in hydrated cements would also yield a barrier impermeable to ionic reactants such as alkali

---

* *Present address*: Massachusetts Institute of Technology, Department of Mechanical Engineering, Cambridge, MA 02139, USA.

0022-2461/92 $03.00 + .12

cations and carbonic acid, HCO_3^-, in a water-wet environment. Therefore, we investigated the effects of water-born organic polymers incorporated into calcium aluminate cements, on the rate of carbonation at high temperature. It is already known that cement mortars and concretes modified with water-born polymers (such as styrene–butadiene, polyacrylic ester, styrene–acrylic ester and ethylene–vinyl acetate emulsions), are less susceptible to carbonation at ambient temperature [8, 9]. The authors reasoned that the solid polymer films formed in the cement matrices effectively fill the small interstices in the hydrated cement pastes, and also act as a protective barrier to prevent the CO_2-laden water from contacting the hydration products.

When cement pastes which contained the organic polymers were exposed in an autoclave at a temperature of ~ 300 °C, it was found that alkaline-earth metals, M (such as calcium and magnesium), that are liberated from the hydrated cement grain surfaces, react preferentially with the ester and carboxylate functionaries located in the main chains and pendents of the polymers [10, 11]. The ionic interactions occurring between the dissociated M cations and the carboxylic anions, COO^-, derived from the alkali-catalysed hydrolysis of the organic functional groups, yield M-bridged ($-COO^-M^{2+-}OOC-$) carboxylate complexes. The presence of these complexes was found to increase the thermal stability in hot air [12, 13].

In our current work, emphasis was given to the relationships between the rate of Na_2CO_3-induced carbonation and the extent and quality of COO–Ca complexity formed in the autoclaved polymer–cement composite systems. Our approach focused on the use of different polymer-incorporated calcium aluminate cement samples after exposure for 24 h in water at 300 °C. These samples were then exposed to a 0.05 M Na_2CO_3–water solution at 300 °C. The rates of carbonation and the resulting strength losses were determined after exposure periods for up to 30 days. These data were then correlated with the phase compositions and transitions in the polymer-modified calcium aluminate cement pastes before and after exposure in the hot Na_2CO_3 solution.

2. Experimental procedure

2.1. Materials

Three water-borne polymers, carboxylated styrene–butadiene (CSB) copolymer, styrene–acrylate (SA) copolymer, and acrylic (AC) polymer emulsion, were used. The total concentration of solid state polymer in these emulsions was ~ 50 wt %. The pH values for the CSB, SA and AC emulsions were ~ 10.5, ~ 8.0 and ~ 2.6, respectively. The acid-type AC polymer contained a certain number of carboxylic acid groups. Contrarily, the structures of the CSB and SA polymers contain a neutralized functional group such as a metal carboxylate or an ester.

Calcium aluminate cement was used as the high-temperature cementing material. A typical chemical composition of the cement is: 46.5 wt % Al_2O_3, 35.5 wt % CaO, 6.0 wt % Fe_2O_3, 8.5 wt % SiO_2, 0.7 wt % MgO and 2.0 wt % SO_3.

The compositions of the polymer-modified cements used in this study are shown in Table I. All of the mixes were designed to yield slurries that were pumpable. The specimens were prepared in accordance with the following sequence. First, in order to produce water-diluted polymer emulsions, the as-received polymers, at solid polymer concentrations ranging from 0%–20% by weight of the total anhydrous cement, were added to an appropriate amount of water and then stirred for 15 min. The diluted emulsions were then thoroughly mixed with the cement. As seen in Table I, the water-to-cement (W/C) ratios in the composite slurries depended primarily on the concentrations of solid polymer; namely, an increase in polymer concentration resulted in a lower W/C ratio. The slurries were then placed in 15 mm diameter and 30 mm long cylindrical moulds which were maintained at room temperature until the cement paste set completely. These specimens and samples powdered by grinding set materials, were then immersed in water at 300 °C for 24 h. The powdered samples were used mainly in measurements of the rate of carbonation, and in determinations of the complexes formed and the phases present. After the hydrothermal treatment, some of the specimens were immersed in 0.05 M Na_2CO_3-laden water at 300 °C.

2.2. Measurements

Infrared spectroscopy was employed as a means of estimating the extent of calcium-complexed polymer formation and for investigating the influence of the complexes on the carbonation of autoclaved cements. The concentration of $CaCO_3$ formed in the cements after exposure to hot 0.05 M Na_2CO_3 solutions was determined using thermogravimetric analysis (TGA) and by measuring the weight loss at which the thermal decompositions of $CaCO_3$ occur over the temperature range 600–770 °C [14]. X-ray powder diffraction (XRD) was used to investigate the phase assemblages and transitions or transformations of the modified and unmodified calcium aluminate cements before and after exposure. The morphological and microstructural features of the hydrated cement products were studied using scanning electron microscopy (SEM).

3. Results and discussion

3.1. COO–Ca complex → $CaCO_3$ conversion

Prior to estimating the carbonation of polymer-modified calcium aluminate cement pastes, interactions occurring between the water-borne polymers and the cements during the autoclave exposure at 300 °C were explored using infrared spectroscopy over the frequency range 1800–1400 cm^{-1}. Polymer-modified cement paste samples containing 50 wt % cement and 50 wt % water-borne polymer were used in this study. Fig. 1 shows infrared spectra for bulk CSB copolymer, a 25 °C-hydrated CSB–cement composite and a CSB–cement composite after exposure for 24 h in an autoclave at 300 °C. A typical infrared spectrum

TABLE I Slurry formulations for polymer-modified and unmodified cement pastes

P/C	W/C	Calcium aluminate cement (g)	Water (g)
0	0.49	67	33.0
0.05	0.32	67	21.4
0.10	0.28	67	18.7
0.15	0.25	67	16.6
0.20	0.24	67	16.1

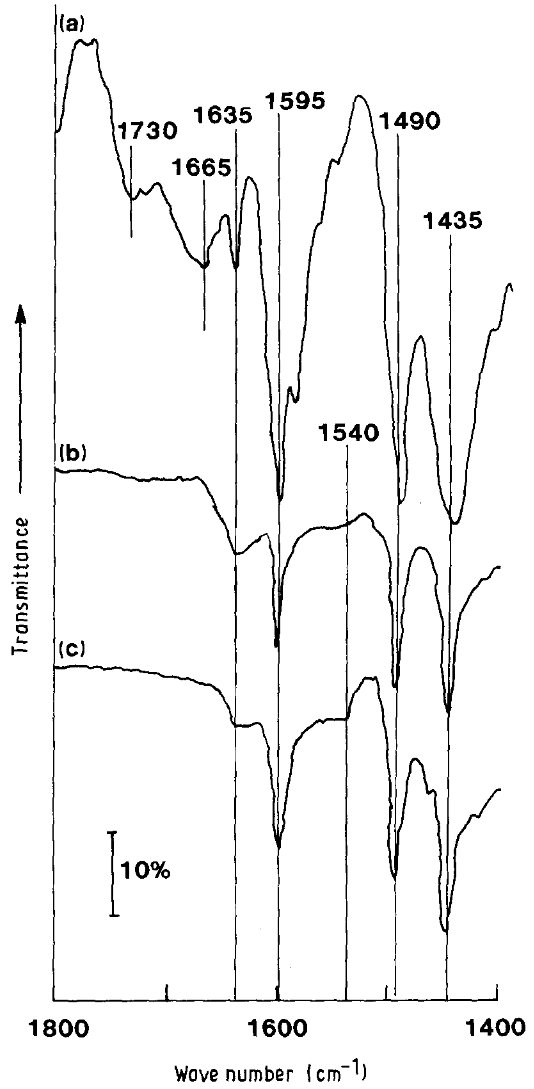

Figure 1 Infrared spectra for (a) bulk CSB copolymer, (b) CSB-modified hydraulic cement at 25 °C, and (c) 300 °C autoclaved CSB–cement composite.

for bulk CSB (Fig. 1a) reveals the carboxylate in the peaks at either 1730 or 1665 cm^{-1}, the diene (C=C) at 1635 cm^{-1}, the aromatic C=C at 1595 and 1490 cm^{-1}, and the aliphatic CH_2 at 1435 cm^{-1}. The spectrum for the CSB-modified cement paste that was cured in water at 25 °C (Fig. 1b) is characterized by the appearance of a slight shoulder peak at 1540 cm^{-1} and considerably diminished intensities for the peaks at 1730 and 1665 cm^{-1}. As seen in Fig. 1c, a pronounced shoulder peak at 1540 cm^{-1} is apparent for the 300 °C autoclaved sample. It is believed that the reason for the formation of the new peak around 1540 cm^{-1} and the reduction in the carboxylate groups in the CBS copolymer, is the formation of a COO–Ca complex yielded through an ionic reaction occurring between the carboxylic anions, COO^-, formed by the alkali-catalysed hydrolysis of carboxylate in the CBS, and the transitional Ca^{2+} ions dissociated from the cement grains.

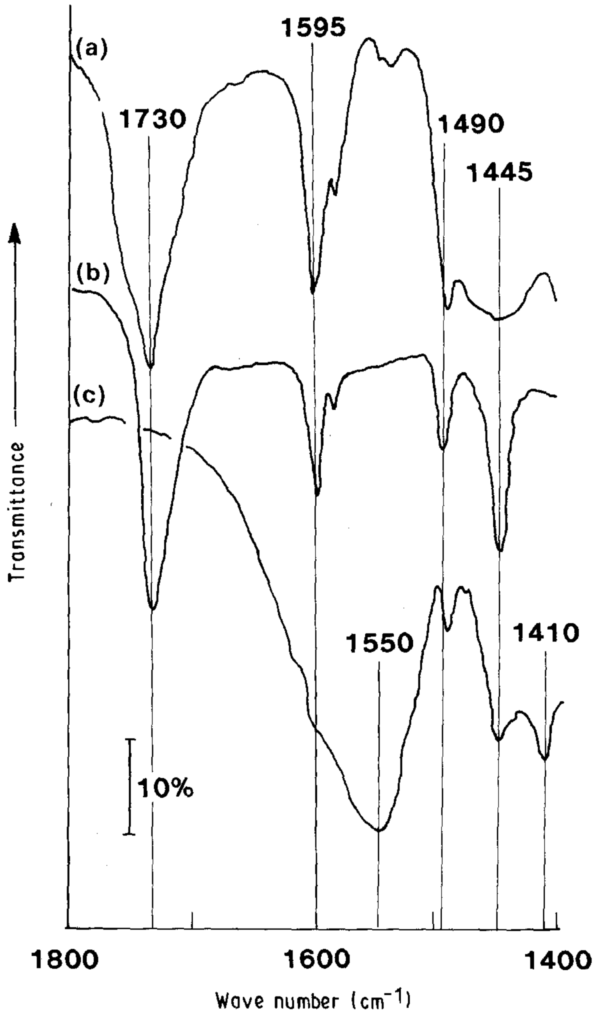

Figure 2 Infrared spectra of (a) bulk SA copolymer, (b) SA-modified hydraulic cement at 25 °C, and (c) SA-modified cement autoclaved at 300 °C.

The infrared spectra for the SA copolymer-modified cement composite series are given in Fig. 2. As mentioned previously, the peaks at 1730, 1595, 1490 and 1445 cm^{-1} for the bulk SA copolymer (Fig. 2a), correspond to the ester groups in acrylate, the aromatic C=C in styrene, and the aliphatic CH_2 in the copolymer, respectively. Spectral features similar to those for the bulk SA are apparent for the 25 °C-hydrated SA–cement composites (Fig. 2b). In contrast, the features displayed by the 300 °C-autoclaved samples (Fig. 2c) were quite different. These differences include the presence of absorption peaks at 1550 and 1410 cm^{-1}, and the disappearance of the peak at 1730 cm^{-1}. A possible interpretation for this is that the autoclave treatment leads to a higher rate for the *in situ* conversion of the functional ester to a COO–Ca complex formation in the cement pastes. Similar trends were observed for the AC-modified cement composite series (see Fig. 3). Namely, the absorption band at 1710 cm^{-1} which is ascribable to the carbonyl groups, C =O, in carboxylic acid, markedly shifts to a position at 1550 cm^{-1} after the composite is exposed in the autoclave at 300 °C (Fig. 3c). Collectively, these results suggest that, although no evidence of COO–Ca complex formation was found at room temperature, autoclave exposure of SA–cement and AC–cement composite systems forms many *in situ* converted COO–Ca complexities. By comparison with the intense peak at 1550 cm^{-1} for the composite systems, the weaker peak in the vicinity of 1540 cm^{-1} for the autoclaved CSB–cement system seems to indicate that the extent of COO–Ca complexities formed in this system is very small.

Particular interest was then placed on the susceptibility of these complex formations to Na_2CO_3-induced carbonation reactions. Initially, we estimated the extent of the complex formation in the 300 °C-autoclaved SA–cement and AC–cement systems by comparing the variations that occur in the 1550 cm^{-1} absorption peak as a function of the concentration of polymer added to the cement paste. These results, summarized in Fig. 4, show that the absorbance value, and therefore the amount of complex formation, increases with an increase in the polymer-to-cement (P/C) ratio. Also, the extent of the complex formation is somewhat larger in the AC system than in the SA one.

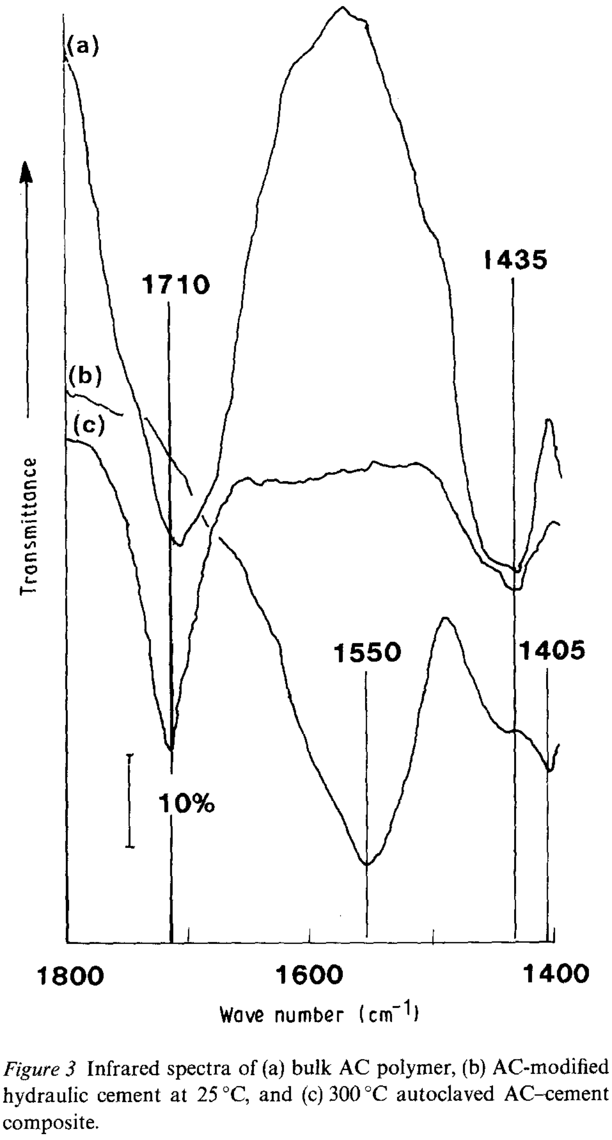

Figure 3 Infrared spectra of (a) bulk AC polymer, (b) AC-modified hydraulic cement at 25 °C, and (c) 300 °C autoclaved AC–cement composite.

Estimates of the conversion rates of the COO–Ca complex to $CaCO_3$ in both the SA and AC systems were then made. For use in this study, 300 °C-autoclaved P/C = 15 specimens were exposed for up to 7 days in a 0.05 M Na_2CO_3–water solution at 300 °C. Because the infrared absorption peak at ~ 1420 cm^{-1} is assigned to the presence of calcite, $CaCO_3$ [15, 16], comparisons of the absorbance ratios between the $CaCO_3$ at 1420 cm^{-1} and COO–Ca at 1550 cm^{-1} are indicative of the COO–Ca → $CaCO_3$ conversion rates. Although it is recognized that the rate of carbonation of the cement hydrates may have an effect on the absorbance at 1420 cm^{-1}, a high absorbance ratio can be assumed to indicate a rapid conversion rate. The results from these specimens are summarized in Fig. 5, and they indicate that the ester-derived complex formations in the SA–cement systems are much more susceptible to alkali carbonation than those formed in the AC–cement systems. Therefore, the latter forms a structure which has a much greater resistance to carbonation. Even though the specimens were exposed for 7 days, the absorbance ratio of this system showed no appreciable change. In contrast, the absorbance ratio for the SA systems increased rapidly with exposure time.

The carbonation reaction of ester-derived COO–Ca complexes in the SA system can be elucidated as follows; initially, the sodium carbonate dissolves in the hot water to form carbonic acid, HCO_3^-, and sodium hydroxide reactants

$$Na_2CO_3 + 2H_2O \rightleftharpoons 2NaOH + H^+ + HCO_3^- \quad (1)$$

When the calcium-bridged COO groups formed in the main chains come in contact with these reactants, the

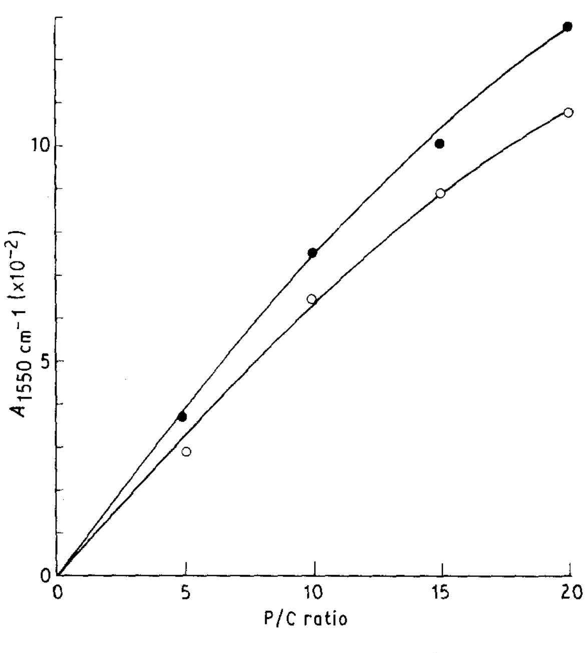

Figure 4 Variations in absorbance at 1550 cm^{-1} with P/C ratios for autoclaved (○) SA–cement and (●) AC–cement systems.

reactive sodium ions will break COO–Ca bonds to form COO–Na complexes and $CaCO_3$. This transformation process is shown in Reaction 2. Therefore, it is possible to assume that the appearance of sodium-complexed products formed by substituting calcium for sodium in conjunction with the formation of $CaCO_3$, results in a chain scission of the SA macromolecules. This may result in a decrease in the mechanical properties of SA–cement composite specimens.

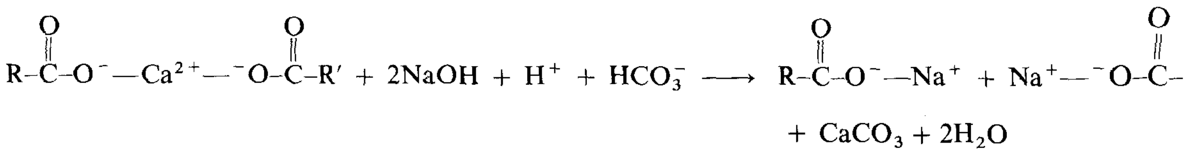

$$\text{R}{-}\overset{\text{O}}{\overset{\|}{\text{C}}}{-}\text{O}^-{-}\text{Ca}^{2+}{-}{}^-\text{O}{-}\overset{\text{O}}{\overset{\|}{\text{C}}}{-}\text{R}' + 2\text{NaOH} + \text{H}^+ + \text{HCO}_3^- \longrightarrow \text{R}{-}\overset{\text{O}}{\overset{\|}{\text{C}}}{-}\text{O}^-{-}\text{Na}^+ + \text{Na}^+{-}{}^-\text{O}{-}\overset{\text{O}}{\overset{\|}{\text{C}}}{-}\text{R}' + \text{CaCO}_3 + 2\text{H}_2\text{O} \qquad (2)$$

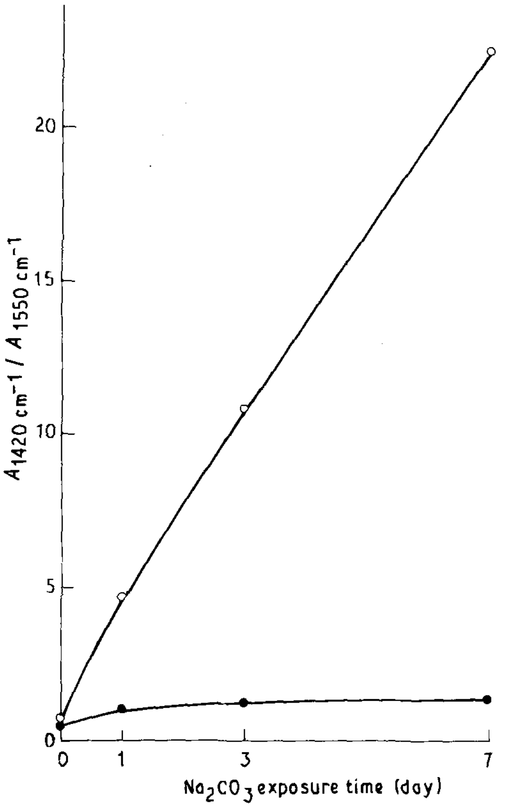

Figure 5 $CaCO_3$ (at 1420 cm^{-1})-to-COO–Ca complex (at 1550 cm^{-1}) absorbance ratios versus Na_2CO_3 exposure times at 300 °C for (○) SA–cement and (●) AC–cement composites having P/C = 15.

Based upon the above information, the studies were extended to determine if changes in compressive strength occur with the degree of COO–Ca → $CaCO_3$ conversion, and to relate any changes with the extent of complex formation in the polymer-modified cement specimens after exposure times up to 30 days in 0.05 M Na_2CO_3-laden water at 300 °C. For use in this work, specimens composed of the slurry formulations listed in Table I were prepared in an autoclave at 300 °C, and they were then exposed to the hot Na_2CO_3 solution. Referring to Fig. 6, the test results indicate that when compared to the controls, all of the specimens containing organic polymers initially had greater strengths. The highest strength (~ 66 MPa) was obtained with AC-modified specimens having a P/C ratio of 15. This value is six times greater than that of the autoclaved controls. The magnitudes of the strength improvements obtained by incorporating the water-borne polymers were in the order AC- > SA > CSB. This indicates that the extent and the

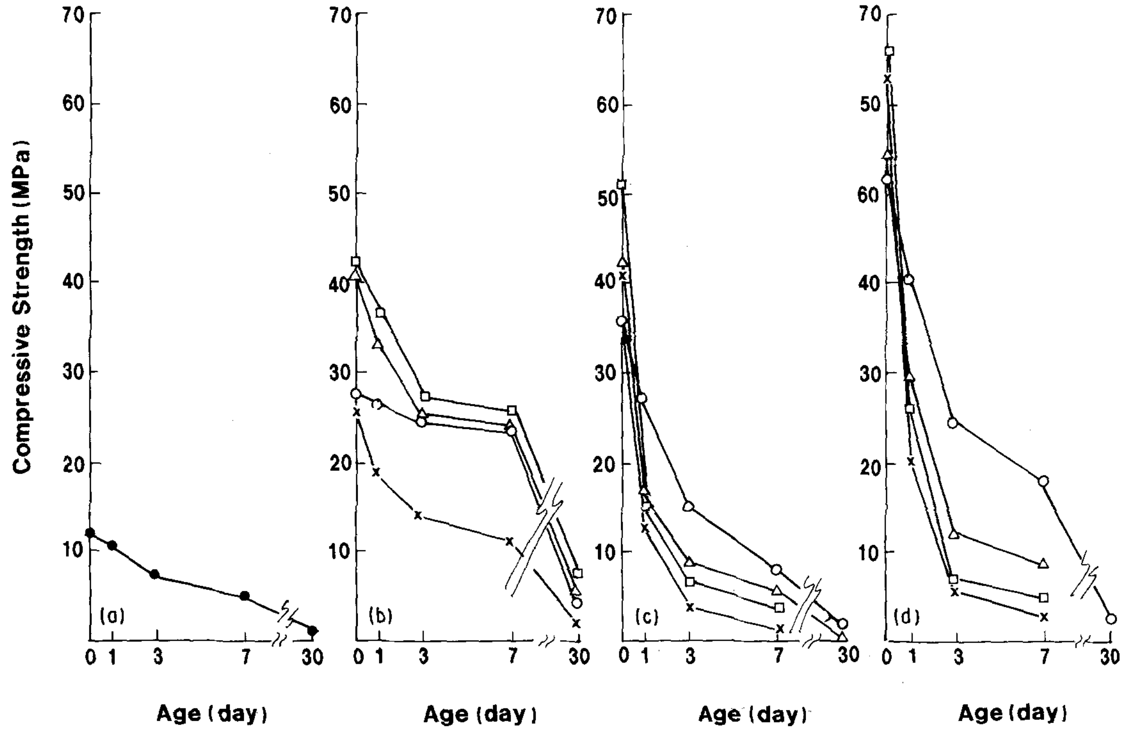

Figure 6 Loss in compressive strength of autoclaved polymer–cement composites and control specimens after exposure to Na_2CO_3-laden solution at 300 °C. P/C = (○) 5, (△) 10, (□) 15, (×) 20. (a) Control, (b) CSB, (c) SA, (d) AC.

conformation of the COO–Ca complexes formed in the autoclaved cement pastes play important roles in establishing the mechanical behaviour of polymer–cement composites. In the case of the former, the larger extent of the complex yielded in the AC and SA composites results in strengths greater than those for the CSB systems which represent a minimum extent of complex formation. With regard to the quality of the complexes, the presence of COO–Ca complex formations derived from carboxylic acid functionaries in AC polymers seems to result in strengths greater than those containing complexes derived from the ester in SA polymers.

Upon exposure of all of the polymer-modified cements to a 300 °C Na_2CO_3 solution, strength losses occurred. The causes for this were associated with two factors: (1) the species of polymer, and (2) the P/C ratio. With the exception of the specimens with a P/C ratio of 5, all of the AC and SA specimens exhibited major strength losses within 3 days. The rate of strength loss increased as the P/C ratio increased. The results from infrared studies on these specimens indicated that the conversion rate of the AC-derived calcium complexes into calcite was considerably lower than that from SA derived ones. Therefore, the rapid loss of strength for the AC specimens may be associated with phase changes in the cement hydration products, and not with alkali carbonation of the COO–Ca complexes and cement hydrates. The rapid reduction in the strength of the SA specimens may be due to a combination of effects such as the carbonation and phase transition of cement hydrates in conjunction with chain breakage of the polymer brought about by replacement of calcium in the complex structures by sodium originating from the presence of Na^+ and HCO_3^- ionic reactants.

Compared to the AC and SA samples, specimens containing the CSB systems exhibited lesser losses after exposure for 7 days. The strength for 7 day aged P/C 15 specimens was $\sim$ 26 MPa, a value five times greater than that of the control at the same age. Although continued exposure to 30 days resulted in a major loss in strength, the value of $\sim$ 8 MPa was considered significant. These data suggest that CSB copolymer films formed in autoclaved cement pastes serve as reinforcement to minimize deterioration caused by carbonation of hydrated cement products at elevated temperatures.

3.2. XRD, TGA and SEM analysis

Studies were conducted to obtain a better understanding of the factors which contribute to the superior strength developed by the autoclaved polymer–cement composites and to the subsequent strength losses which occur upon exposure to Na_2CO_3. In this effort, polymer modified and unmodified specimens were analysed before and after exposure for up to 30 days in Na_2CO_3 solutions at 300 °C using the combined analytical techniques of XRD, TGA and SEM. These studies evaluated the phase compositions and conversions, the quantity of calcite, and the morphological and microstructural features of the hydrated cement products before and after exposure.

The XRD data (see Table II) were summarized by compiling the X-ray peak area for each phase formed in the specimens as a function of the Na_2CO_3 exposure time. Prior to discussing the results, it should be noted that the goal of the XRD study was not to quantify the amount of each phase formed at the various exposure times, but to comprehend the phase relations which associate with strength development and loss. For the control specimens, identified P/C = 0, the major hydration product formed within the 300 °C autoclaved specimens before exposure was biccholite, $Ca_2Al_2SiO_6(OH)_2$. Boehmite (γ-AlOOH), triclinic anorthite ($CaAl_2SiO_2O_8$), calcite ($CaCO_3$), gehlenite, ($Ca_2Al_2SiO_7$), and corundum (α-Al_2O_3), were present as secondary crystalline products. With regard to the presence of $CaCO_3$, this is commonly derived from the alkali carbonation reaction of calcium-based hydration products with carbonic acid (HCO_3^-) which is formed by the dissolution of Na_2CO_3 in an autoclave environment. However, in this case because a certain amount of $CaCO_3$ was already present in the specimens, there is no evidence that the hydration products preferentially reacted with dissociated HCO_3^- to form $CaCO_3$. This reflects directly on a question as to whether the presence of γ-AlOOH and α-Al_2O_3 phases is related to a by-product of carbonation. Unfortunately, the limits of the data prevent answering that question.

After exposure of the control specimens to the hot Na_2CO_3 solution for 7 days, the XRD tracings exhibited enhanced peak areas for all of these phases. In particular, the peak area for calcite increased greatly. Extension of the exposure time to 30 days resulted in changes in the phase assemblages and species. These include the presence of gehlenite as a principal phase, the formation of wairakite [$Ca(Al_2Si_4)O_{12} \cdot 2H_2O$] and hexagonal anorthite ($CaAl_2Si_2O_8$), and the disappearance of the boehmite, triclinic anorthite, biccholite and corundum phases. The reason for the formation of wairakite and the disappearance of biccholite is the phase transformation of biccholite to wairakite. Also, long-term exposure is favourable for the triclinic → hexagonal anorthite phase transition. When compared with that for the 7 day aged specimens, the peak area for calcite was reduced. This implies that a certain amount of $CaCO_3$ was eliminated during exposure for 30 days.

The quantity of $CaCO_3$ formed was estimated from TGA data and measurements of the weight loss resulting from the thermal decomposition of $CaCO_3$ over the temperature range 600–770 °C. The TGA data are given in Fig. 7. It can be seen that the greatest amount of $CaCO_3$ in the controls was in the 7 day aged specimens, and that there was a considerable reduction after 30 days. These results are in agreement with the results obtained from the XRD analyses. Thus, a possible interpretation for the reduction of $CaCO_3$ concentration after ageing for 30 days is the conversion of calcite into water-soluble calcium bicarbonate [$Ca(HCO_3)_2$]. As is well known [17], the formation of

TABLE II Changes in X-ray peak area for phases formed in 300 °C autoclaved unmodified and modified calcium aluminate cement pastes as a function of exposure *time in* Na_2CO_3-laden water at 300 °C

Polymer[a]	P/C	Test age (day)	Boehmite, γ-AlOOH (0.611 nm)	Wairakite, $Ca(Al_2Si_4)O_{12}\cdot 2H_2O$ (0.341 nm)	Hexagonal anorthite, $CaAl_2Si_2O_8$ (0.32 nm)	Triclinic anorthite, $CaAl_2Si_2O_8$ (0.319 nm)	Calcite, $CaCO_3$ (0.304 nm)	Gehlenite, $Ca_2Al_2SiO_7$ (0.285 nm)	Biccholite, $Ca_2Al_2SiO_6(OH)_2$ (0.279 nm)	Corundum, α-Al_2O_3 (0.209 nm)
–	0	0	0.8	0.0	0.0	0.8	0.5	0.4	1.7	0.9
–	0	7	1.2	0.0	0.0	1.2	1.1	0.6	2.3	1.2
–	0	30	0.0	0.7	0.3	0.0	0.7	1.7	0.0	0.0
CSB	5	0	0.5	0.0	0.0	0.6	0.4	2.1	0.8	0.5
CSB	5	7	1.5	0.0	0.0	1.2	0.7	2.2	2.6	1.7
CSB	5	30	0.0	0.2	0.6	0.6	0.5	2.5	0.9	0.5
CSB	15	0	0.8	0.0	0.0	0.7	0.5	1.3	1.8	1.1
CSB	15	7	1.9	0.0	0.0	1.8	1.1	1.5	1.9	1.2
CSB	15	30	0.7	0.4	1.3	0.9	0.8	1.6	1.5	0.9
SA	5	0	0.5	0.0	0.0	0.5	0.4	3.2	0.9	0.5
SA	5	7	0.8	0.3	0.0	0.7	1.9	2.0	1.0	1.0
SA	15	0	0.6	0.0	0.0	0.5	0.3	3.1	0.8	0.8
SA	15	7	1.1	0.4	0.0	0.7	2.3	1.7	0.7	0.8
AC	5	0	0.6	0.0	0.0	0.5	0.4	0.8	1.6	1.0
AC	5	7	0.4	1.0	1.1	0.4	0.6	1.3	1.4	0.9
AC	15	0	0.7	0.0	0.0	0.6	0.3	1.4	1.9	1.1
AC	15	7	0.5	1.7	0.7	0.5	0.4	1.6	1.7	1.0

[a] CSB, carboxylated styrene–butadiene copolymer; SA, styrene–acrylate copolymer; AC, acrylic polymer.

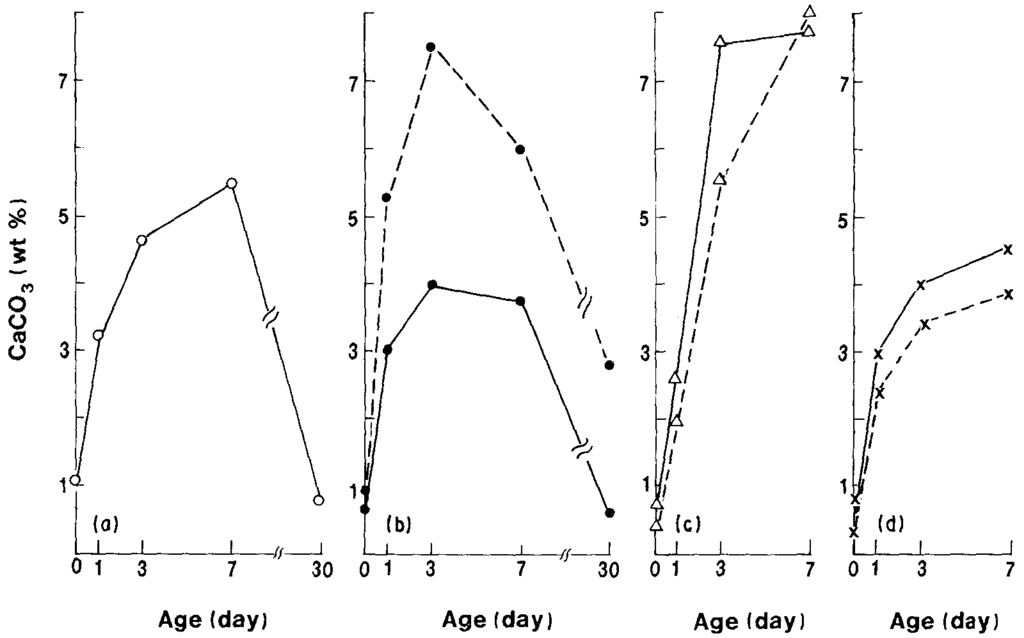

Figure 7 Changes in $CaCO_3$ concentration formed in aged controls and composite specimens. P/C: (——) 5, (– – –) 15. (a) Control, (b) CSB, (c) SA, (d) AC.

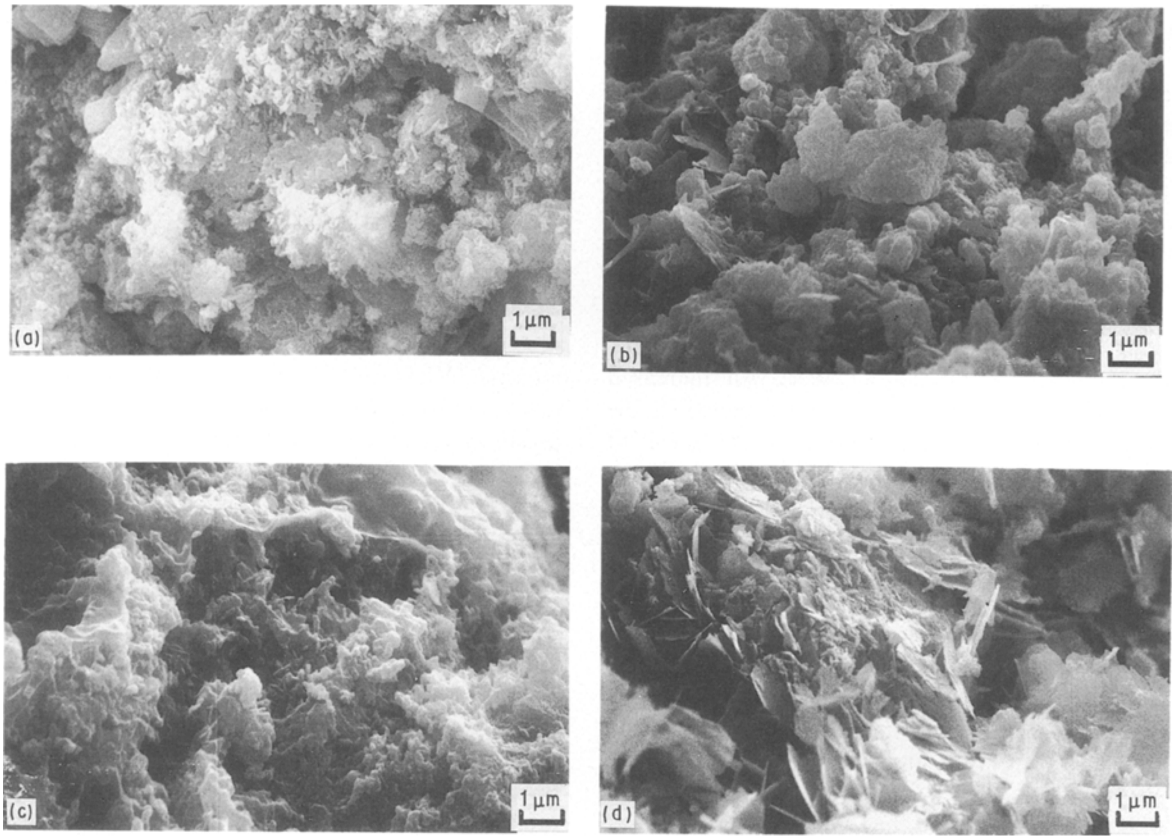

Figure 8 Scanning electron micrographs of unmodified cement and CSB-modified cement (P/C = 15) before and after exposure for 30 days to Na_2CO_3-laden water at 300 °C. (a) Unexposed control, (b) exposed control, (c) unexposed CSB-cement composite, and (d) exposed composite.

calcium bicarbonate salt refers to the reaction with its favourable equilibrium

$$CaCO_3 + H^+ + HCO_3^- \rightleftharpoons Ca(HCO_3)_2 \quad (3)$$

Once such a soluble salt forms in a hydraulic cement matrix, it is predictable that the microstructure of the cement paste will become more porous, thereby reducing the compressive strength. This was supported by the results from SEM analyses of the fractured surfaces of the autoclaved controls before and after exposure for 30 days. As can be seen in these scanning electron micrographs (Fig. 8a and b), the image of the exposed specimen (Fig. 8b) is characterized by a porous microtexture and the presence of a flake-like crystal. This is in contrast with the appearance of the unexposed one (Fig. 8a). Hence, the strength loss for the Na_2CO_3-exposed controls is likely to be associated with an increase in porosity caused by the formation of $Ca(HCO_3)_2$ salt, rather than phase change-type strength retrogression which is represented by biccholite → wairakite and triclinic → hexagonal anorthite phase conversions.

Based upon the above evidence, our experimental work was then focused on obtaining a full understanding of the factors affecting the strength loss of the exposed polymer–cement composites. As described in the previous section on infrared analyses and compressive strength measurements, the rate of COO–Ca → $CaCO_3$ conversion and the magnitude of strength development for the autoclaved composite specimens depends upon the conformation and the extent of COO–Ca complexity yielded at the interface between the polymer and the cement. The complex formation which contributed the most to strength development and was the least susceptible to carbonation was found to be derived from carboxylic acid in the AC polymer. Thus, it is important to not only understand the behaviour of this complex within composite materials, but also how the phase compositions and the carbonation rates of the cement hydration products in the presence of these complexes affect the strength. Because the autoclaved AC–cement composites having a $P/C = 15$ exhibited the highest strengths in this test series, emphasis was placed on identification of the phases responsible for the strength development in this composite. Such identification was made by comparing the phase compositions in the AC composite and the control. These results are summarized in Table II. Although both samples contained many of the same phases, the AC specimen had a relatively large peak area of gehlenite, which therefore is the major phase. An increased amount of gehlenite phase was also detected in the SA- and CSB-modified cement systems. This seems to suggest that the high strength developed in the autoclaved composite is not only due to the quality and extent of COO–Ca formation, but also to the presence of a well-formed gehlenite phase. Based upon the results described above, it appears that the magnitude of the expected strength loss can be made by comparisons of the gehlenite mass fraction, the biccholite → wairakite and triclinic → hexagonal anorthite conversion rates, and the degree of carbonation of the composite and control specimens after exposure.

For samples containing the CSB copolymer at $P/C = 5$ and 15, trends for the variation in XRD peak area for each phase as a function of the exposure age, were similar to those of the control. Exceptions were a decreased biccholite → wairakite transformation and an increased triclinic → hexagonal anorthite phase transition in the 30 day aged specimens. As can be seen in the TGA data (Fig. 7), the $CaCO_3$ concentration in both the $P/C = 5$ and 15 specimens increased during exposures up to 3 days. It then decreased. This implies that the $CaCO_3 \rightarrow Ca(HCO_3)_2$ conversion occurs after 3 days exposure. The conversion rate into $Ca(HCO_3)_2$ for the 30 day exposed specimens was not significantly different from that of the controls. The data also suggest that the addition of a large amount of CSB copolymer to the cement pastes results in an enhanced carbonation rate.

Alterations in the morphological features of $P/C = 15$ specimens that occur upon exposure for 30 days were also evaluated. A micrograph is shown in Fig. 8d. Compared to the surface before exposure (Fig. 8c), partially agglomerated flake-like crystals are apparent. These result in increased porosity. The major causes for the formation of such a porous structure which relates directly to the strength loss, are (1) a high conversion rate of $CaCO_3$ to $Ca(HCO_3)_2$, and (2) an enhanced triclinic → hexagonal anorthite transition. In addition, alkali-catalysed hydrothermal disintegration of the polymer itself may occur upon long-term exposure. However, no study of this was made.

In the case of the aged SA–cement and AC–cement composites, the phase composition analyses were performed only on 7 day-aged specimens. For the exposed SA composites ($P/C = 5$ and 15), the phase assemblage data (Table II) show the presence of wairakite, a greatly increased peak area for $CaCO_3$, and a reduction in the amount of the gehlenite phase. Because wairakite was not detected in the same aged control and CSB specimens, the biccholite → wairakite transformation in the SA composites appears to occur within an exposure time of 7 days. The enhanced carbonation is almost certainly due to the conversion of both the COO–Ca complexes and the cement hydration products into $CaCO_3$. As anticipated, the TGA data indicated a progressive increase in the $CaCO_3$ concentration throughout the 7 day exposure period. These data are plotted in Fig. 7. In contrast, XRD and TGA data indicated a relatively lower carbonation rate for aged AC–cement composite systems, particularly for $P/C = 15$ specimens. It is believed that the formation of a calcium-complexed polymer which has a low susceptibility to alkali carbonation acts to inhibit the carbonation reaction of the cement hydration products. Unfortunately, this carbonation barrier complex film results in the production of a great amount of wairakite and hexagonal anorthite phases, both of which are detrimental for strength development in cement pastes. On the other hand, no appreciable differences between the microstructure features of SA and AC composite specimens, before (Fig. 9a and b) and after (Fig. 9c and d) exposure, were found. As a result, it was not possible to explain satisfactorily the influence of the altered microstructure on the strength reduction of exposed specimens.

4. Conclusions

The findings from our study lead to the following generalized conclusions.

1. The autoclave treatment at 300 °C of calcium aluminate cement pastes modified with water-borne polymers such as carboxylated styrene–butadiene (CSB), styrene–acrylate (SA), and acrylic (AC) emulsions produces significant improvements in compressive strength, particularly for SA–cement and

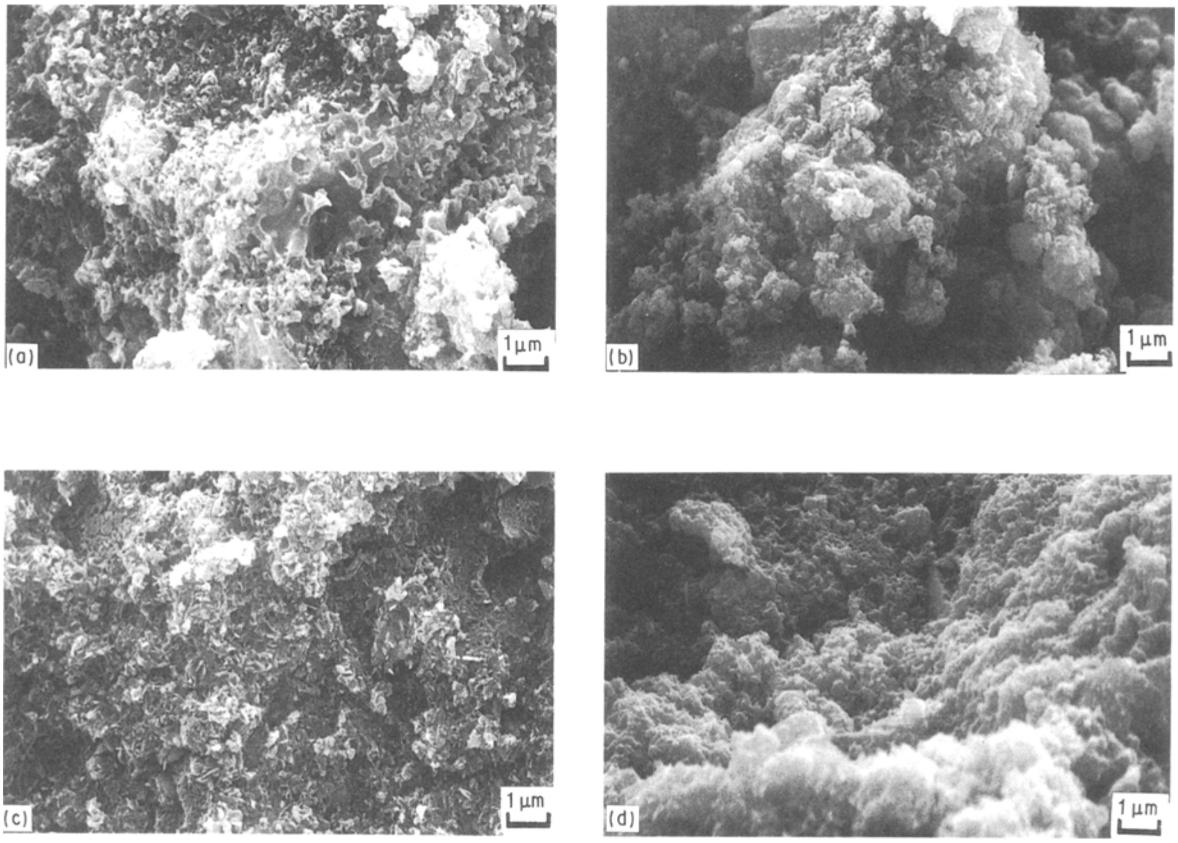

Figure 9 Microstructure views of SA- and AC-modified cement composites before and after exposure for 7 days to 300 °C Na_2CO_3 solution. (a) Unexposed and (b) exposed SA composites, and (c) unexposed and (d) exposed AC composites.

AC–cement composites. This is due to the formation of a calcium-complexed carboxylate polymer structure at the interface between the polymer and the cement, and the presence of a well-formed gehlenite phase in the composites.

2. When the COO–Ca complex formations were subjected to alkali carbonation reactions in the presence of Na^+ and HCO_3^- ionic reactants at 300 °C, the rates of COO–Ca $\rightarrow$ $CaCO_3$ conversion depended primarily on the different conformations of the complex structure. Namely, a complex formation derived from the pendent carboxylic acid of AC polymer results in a structure highly resistant to alkali carbonation. In contrast, as a result of the substitution of sodium for calcium in the complex, the ester (SA polymer)-derived complex was found to be very susceptible to alkali carbonation.

3. The calcium-complexed polymer structure formed in AC–cement composites serves to inhibit the carbonation reaction of cement hydration products. Unfortunately, the formation of this carbonation barrier produces a larger amount of transformed wairakite and hexagonal anorthite phases, resulting in a decline in mechanical properties.

4. The considerable loss in strength for the autoclaved calcium aluminate cement pastes after exposure to a Na_2CO_3 solution at 300 °C was attributed to the creation of a porous microstructure brought about by the conversion of $CaCO_3$ into water-soluble $Ca(HCO_3)_2$, and bicchołite → wairakite transformations.

5. The major reasons for the loss of strength in SA–cement composites appear to be (i) chain breakage of the SA polymer by a COO–Ca → COO–Na transforming reaction in connection with the COO–Ca $\rightarrow$ $CaCO_3$ conversion, and (ii) the shift to a minor phase of gehlenite crystal contributing to strength development.

6. Despite the strength reduction caused by $CaCO_3 \rightarrow Ca(HCO_3)_2$ conversion and the triclinic → hexagonal anorthite phase transition, CSB–cement composites with a $P/C = 5$ were identified as promising composite systems for use in hydrothermal fluids containing CO_2. Experiments to measure the kinetics at lower temperatures are planned.

Acknowledgement

This work was performed under the auspices of the US Department of Energy, Washington, DC, under Contract no. DE-AC02-76CH00016.

References

1. N. B. MILESTONE, T. SUGAMA, L. E. KUKACKA and N. CARCIELLO, *Cem. Concr. Res.* **16** (1986) 941.
2. *Idem, ibid.* **17** (1987) 37.
3. *Idem, ibid.* **17** (1987) 295.
4. R. A. BRUCKDORFER, Carbon Dioxide Corrosion Resistance in Cements, in "Proceedings of the 1985 Annual Southwestern Petroleum Short Course", Lubbock USA, 23–25 April 1985.

5. H. G. MIDGLEY and A. MIDGLEY, *Mag. Concr. Res.* **27** (1975) 59.
6. R. D. BLENKINSOP, B. R. CURRELL, H. G. MIDGLEY and J. R. PARSONAGE, *Cem. Concr. Res.* **15** (1985) 276.
7. *Idem, ibid.* **15** (1985) 385.
8. K. H. ANGELMAYER, *KunstharzNachr* **17** (1982) 1.
9. K. OKADA and Y. OHAMA, in "Proceedings of 5th International Congress on Polymers in Concrete", edited by B. W. Staynes, Brighton, 22–24 Sept. 1987, pp. 13–17.
10. T. SUGAMA, L. E. KUKACKA and W. HORN, *J. Mater. Sci.* **15** (1980) 1498.
11. *Idem, Cem. Concr. Res.* **11** (1981) 429.
12. *Idem, J. Appl. Polym. Sci.* **24** (1979) 2121.
13. T. SUGAMA and L. E. KUKACKA, *Cem. Concr. Res.* **12** (1982) 789.
14. W. W. WENDLANDT, "Thermal Methods of Analysis", 2nd Edn (Wiley, New York, 1974) p. 16.
15. M. PEREZ, T. VAZQUEZ and F. TRIVINO, *Cem. Concr. Res.* **13** (1983) 759.
16. R. A. NYQUIST and R. O. KAGEL, "Infrared Spectra of Inorganic Compounds" (Academic Press, New York, 1971) p. 79.
17. F. M. LEA, "The Chemistry of Cement and Concrete" (Arnold, London, 1956) p. 288.

Received 23 August 1990
and accepted 28 February 1991